# Structure of $Ca^{2+}$ Prothrombin Fragment 1 Including the Conformation of the Gla Domain†

Manuel Soriano-Garcia,‡ Chang H. Park,§ A. Tulinsky,* K. G. Ravichandran, and Ewa Skrzypczak-Jankun
*Department of Chemistry, Michigan State University, East Lansing, Michigan 48824*
*Received May 30, 1989; Revised Manuscript Received July 3, 1989*

ABSTRACT: The structure of $Ca^{2+}$ prothrombin fragment 1 has been solved at 2.8-Å resolution by X-ray crystallographic methods. Most of the Gla domain of fragment 1 (residues 1–48), which is highly homologous with the N-terminal regions of six other blood proteins, cannot be identified in the electron density map of the apo structure. This is not the case when crystals are grown in the presence of $Ca^{2+}$ ions where the Gla domain exhibits a well-defined folded structure. The folding of the Gla domain is dominated by secondary structure: (a) 3.0 turns of $\alpha$-helix (25%) and (b) five short $\beta$-strands arranged into two $\beta$-structural units (40%). The Cys18–Cys23 disulfide of the small conserved loop of Gla domains is close to a cluster of conserved aromatic residues. The resulting interaction is probably responsible for the fluorescence quenching event accompanying $Ca^{2+}$ ion binding. Since the Gla domain approximates a discoid, all the Gla residues are easily accessible to solvent. The arrangement of the paired Gla residues (7–8, 20–21, 26–27) is highly suggestive in that they essentially line one edge of the Gla domain creating a potentially intense electronegative environment. This region might well be that associated with phospholipid binding. The kringle structure of $Ca^{2+}$ fragment 1 is essentially indistinguishable from that of the apoprotein at this stage.

Residues 1–48 of prothrombin (Figure 1) are homologous with the comparable N-terminal sequences of factors VII, IX, and X and the proteins designated C, S, and Z (Table I). All contain $\gamma$-carboxy-Glu residues produced by posttranslational modification of Glu by a vitamin K dependent carboxylase. The Gla[1] residues vary in total number from 9 to 12, of which the first 10 are highly conserved. The function of these N-terminal 48 residues is phospholipid binding in the presence of $Ca^{2+}$ ions, and they have become known as the Gla domain, which displays about 65–70% conservation (32–34 residues) among the seven homologous N-terminal regions (Table I).

The Gla domain of prothrombin is utilized in the formation of the prothrombinase complex with factors Va and Xa by binding to the phospholipid membrane in the presence of $Ca^{2+}$ ions (Nelsestuen et al., 1974; Stenflo et al., 1974; Bajaj et al., 1975). The Gla residues of the domain confer the metal ion binding properties common to this class of calcium binding proteins. Ten ions are bound in general with prothrombin (Deerfield et al., 1987a) but only six or seven with one of its proteolytic motifs with thrombin, prothrombin fragment 1 (156 N-terminal residues of prothrombin) (Nelsestuen et al., 1981), with the Gla domain undergoing an accompanying conformational change demanded of membrane binding as evidenced by intrinsic fluorescence quenching (Nelsestuen, 1976; Prendergast & Mann, 1977) and CD measurements (Bloom & Mann, 1978). However, a much smaller number of ions induce the conformational change, and their sites display higher affinity for metal ion binding (Nelsestuen et al., 1981). It has been proposed that the conformational change proceeds via two conformational transitions, one of which is not cation specific while the other is highly selective (Borowski et al., 1986). Comparison of $Ca^{2+}$ and $Mg^{2+}$ ion binding to prothrombin fragment 1 indicates that $Ca^{2+}$ ions bind at three high-affinity, cooperative sites and several noninteracting sites, while the $Mg^{2+}$ ion shows fewer binding sites of less overall binding affinity and significantly less cooperativity (Deerfield et al., 1987b).

In the absence of $Ca^{2+}$ ions, about three-fourths of the Gla domain (Ala1–Leu35) of fragment 1 is disordered in crystals as are the two polysaccharide chains of the molecule (Tulinsky et al., 1988). However, the remaining residues of the Gla domain are ordered with Asp39–Ala47 forming about 2.5 turns of $\alpha$-helix. Diffusing $Ca^{2+}$ ions into crystals of apo fragment 1 produces highly significant intensity changes in the diffraction pattern, but the soaking procedure severely impairs the diffracting ability of crystals, which ultimately disappears in about 1 week (Tulinsky & Park, 1988). However, this is not the case when crystals of fragment 1 are grown in the presence of $Ca^{2+}$ ions (Olsson et al., 1982) where it appears that the Gla domain is structurally ordered. Since the crystallography of $Ca^{2+}$ fragment 1 by Olsson et al. (1982) was conducted at low resolution and resulted only in a balsa wood model, we initiated a program aimed at determining the structure of these crystals at high resolution. As a result, we confirm here that the Gla domain is ordered in such crystals and report its structure at 2.8-Å resolution.

## Materials and Methods

Crystals of $Ca^{2+}$ fragment 1 were grown by the hanging drop method basically according to the conditions described by Olsson et al. (1982): 0.1 M cacodylate buffer, pH 6.5, and 8% (w/v) PEG 6000 in the presence of 100 mM $Ca^{2+}$ ion in the drop with an identical well solution except for 16% PEG 6000 and 200 mM $Ca^{2+}$ ion.[2] The crystals grow slowly, eventually appearing within about 6–9 months. The crystals are orthorhombic, $a$ = 39.39 (4) Å, $b$ = 53.88 (4) Å, and $c$ = 129.60 (8) Å, with space group $P2_12_12_1$, four molecules/unit

† This work was supported by NIH Grant HL25942.
‡ Permanent address: Instituto de Quimica, UNAM, Circuito Exterior, Cd. Universitaria, Mexico D.F. 04510, Mexico.
§ Permanent address: Abbott Laboratories, Abbott Park, IL 60064.

[1] Abbreviations: Gla, $\gamma$-carboxyglutamic acid; CD, circular dichroism; SIR, single isomorphous replacement; ISIR, iterative SIR; ANS, 1-anilinonaphthalene-8-sulfonate.

[2] We thank Dr. G. L. Nelsestuen for providing an abundant supply of bovine fragment 1.

0006-2960/89/0428-6805$01.50/0 

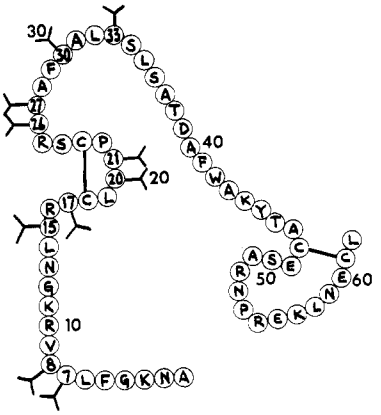

FIGURE 1: Sequence of the Gla domain of prothrombin fragment 1 (1–48) and its accompanying disulfide loop. Gla residues are numbered and designated with a Y.

Table I: Homologous N-Terminal Sequences of the Gla Domain of Prothrombin (1–48)[a]

| | 1 | | | | | | | | 9 | | | | | | | | | | | | 18 |
|---|---|---|---|---|---|---|---|---|---|---|---|---|---|---|---|---|---|---|---|---|---|
| b-prothrombin | A | N | K | G | F | L | γ | γ | V | R | K | G | N | L | γ | R | γ | C |
| h-prothrombin | A | N | T | - | F | L | γ | γ | V | R | K | G | N | L | γ | R | γ | C |
| h-Factor VII | A | N | A | - | F | L | γ | γ | L | R | P | G | S | L | γ | R | γ | C |
| b-Factor IX | Y | N | S | G | K | L | γ | γ | F | V | Q | G | N | L | γ | R | γ | C |
| h-Factor IX | Y | N | S | G | K | L | γ | γ | F | V | Q | G | N | L | γ | R | γ | C |
| b-Factor X | A | N | S | - | F | L | γ | γ | V | K | Q | G | N | L | γ | R | γ | C |
| h-Factor X | A | N | S | - | F | L | γ | γ | M | K | K | G | H | L | γ | R | γ | C |
| b-protein C | A | N | S | - | F | L | γ | γ | L | R | P | G | N | V | γ | R | γ | C |
| h-protein C | A | N | S | - | F | L | γ | γ | L | R | H | S | S | L | γ | R | γ | C |
| b-protein S | A | N | T | - | L | L | γ | γ | T | K | K | G | N | L | γ | R | γ | C |
| h-protein S | A | N | S | - | L | L | γ | γ | T | K | Q | G | N | L | γ | R | γ | C |
| b-protein Z | A | G | S | V | L | L | γ | γ | L | F | γ | G | H | L | γ | K | γ | C |

| | 19 | | | | | | | 27 | | | | | | | | 35 |
|---|---|---|---|---|---|---|---|---|---|---|---|---|---|---|---|---|
| b-prothrombin | L | γ | γ | P | C | S | R | γ | γ | A | F | γ | A | L | γ | S | - | L |
| h-prothrombin | V | γ | γ | T | C | S | Y | γ | γ | A | F | γ | A | L | γ | S | - | S |
| h-Factor VII | K | γ | γ | Q | C | S | F | γ | γ | A | R | γ | I | F | K | D | - | A |
| b-Factor IX | M | γ | γ | K | C | S | F | γ | γ | A | R | γ | V | F | γ | N | - | T |
| h-Factor IX | M | γ | γ | K | C | S | F | γ | γ | A | R | γ | V | F | γ | N | - | T |
| b-Factor X | L | γ | γ | A | C | S | L | γ | γ | A | R | γ | V | F | γ | D | - | A |
| h-Factor X | M | γ | γ | T | C | S | Y | γ | γ | A | R | γ | V | F | γ | D | - | S |
| b-protein C | S | γ | γ | V | C | γ | F | γ | γ | A | R | γ | I | F | Q | N | - | T |
| h-protein C | I | γ | γ | I | C | D | F | γ | γ | A | K | γ | I | F | Q | N | - | V |
| b-protein S | I | γ | γ | L | C | N | K | γ | γ | A | R | γ | I | F | γ | N | N | P |
| h-protein S | I | γ | γ | L | C | N | K | γ | γ | A | R | γ | V | F | γ | N | D | P |
| b-protein Z | W | γ | γ | I | C | V | Y | γ | γ | A | R | γ | V | F | γ | D | - | D |

| | 36 | | | | | | | | 44 | | | | | | | 48 |
|---|---|---|---|---|---|---|---|---|---|---|---|---|---|---|---|---|
| b-prothrombin | S | A | T | D | A | F | W | A | K | Y | T | A | - | - | - | C |
| h-prothrombin | T | A | T | D | V | F | W | A | K | Y | T | A | - | - | - | C |
| h-Factor VII | γ | R | T | K | L | F | W | I | S | Y | S | D | G | D | Q | C |
| b-Factor IX | γ | K | T | T | γ | F | W | K | Q | Y | V | D | G | D | Q | C |
| h-Factor IX | γ | K | T | T | γ | F | W | K | Q | Y | V | D | G | D | Q | C |
| b-Factor X | γ | Q | T | D | γ | F | W | S | K | Y | K | D | G | D | Q | C |
| h-Factor X | γ | K | T | N | γ | F | W | N | K | Y | K | D | G | D | Q | C |
| b-protein C | γ | D | T | M | A | F | W | S | F | Y | S | D | G | D | Q | C |
| h-protein C | Q | D | T | L | A | F | W | S | K | H | V | D | G | D | Q | C |
| b-protein S | γ | - | T | E | Y | F | Y | P | K | Y | L | G | - | - | - | C |
| h-protein S | γ | - | T | D | Y | F | Y | P | K | Y | L | V | - | - | - | C |
| b-protein Z | γ | T | T | D | γ | F | W | R | T | Y | M | G | G | S | P | C |

[a] b, bovine; h, human. b-Prothrombin (Magnusson et al., 1975); h-prothrombin (Degen et al., 1983); h-factor VII (Hagen et al., 1986; b-factor IX (Katayama et al., 1979); h-factor IX (Kurachi & Davie, 1982); b-factor X (Enfield et al., 1980); h-factor X (Fung et al., 1985); b-protein C (Fernlund & Stenflo, 1982); h-protein C (Plutzky et al., 1986); b-protein S (Dahlback et al., 1986); h-protein S (Lundwall et al., 1986); b-protein Z (Hojrup et al., 1985). Gla = γ; obvious deviations from conservation are enclosed by diamonds.

cell, 60% solvent, but unlike the apoprotein, they diffract X-rays well to about 2.0-Å resolution. A set of intensity data was measured at 2.8-Å resolution (5500 reflections observed of 6600, 83%) by using a Wyckoff step-scan procedure with a Nicolet P3/F diffractometer , and an attempt was made to solve the structure by molecular replacement rotation–translation methods utilizing the refined coordinates of apo fragment 1 (Tulinsky et al., 1988). The procedure produced an electron density map which indicated that the Gla domain was ordered and that the α-helix of the apoprotein had shifted in position; however, the density for the Gla domain contained many breaks and was far from being unambiguous. Therefore, the best heavy atom isomorphous derivative of apo fragment 1 (mercury acetate) was prepared with $Ca^{2+}$ fragment 1 crystals (Tulinsky et al., 1988). The derivative proved to have two heavy atom sites with occupancies of about 1.0 and 0.31 ($R_{obs} = \sum||F_{PH}| - |F_P||/\sum|F_P| = 0.12$), similar to the corresponding mercury acetate derivative of the apoprotein (Tulinsky et al., 1985). Moreover, the position of the major mercury site appeared in the vicinity of His96 of the molecular replacement kringle (three disulfide, triple loop structure of residues 66–144) of $Ca^{2+}$ fragment 1 where it was also observed to be in the apo fragment 1 derivative, thus independently supporting the correctness of the separately derived rotation–translation results. Solvent-flattened SIR phases (Wang, 1985) were then combined (Hendrickson & Lattman, 1970) with those obtained by molecular replacement using the kringle structure alone. Again, although molecular replacement with only the kringle of the apo fragment 1 structure (about 50% of the total, but much less if disordered carbohydrate is considered) combined with SIR phases did not bring out the Gla-domain electron density sufficiently for a straightforward interpretation and tracing of the folding, it nonetheless clearly confirmed that the 2.5 turns of α-helix of the apo structure had pivoted around Cys48–Cys61 as a unit by about 30° toward the kringle domain. This led us to include the complete apo fragment 1 structure in molecular replacement phase calculations.

Table II: Combined SIR–Molecular Replacement Refinement Statistics

| indicator[a] | initial | final |
|---|---|---|
| $\langle m \rangle$ | 0.59 | 0.87 |
| $R$ | 0.48 | 0.15 |
| $\langle \Delta\varphi \rangle_{cyl}$ (deg) | | 2.3 |
| $\langle \Delta\varphi \rangle_{inv}$ (deg) | | 8.6 |
| $\langle \lvert\varphi_i - \varphi_f\rvert \rangle$ (deg) | | 61 |
| correlation | 0.83 | 0.98 |

[a] $\langle m \rangle$, average figure of merit; $R = \sum||F_o| - |F_c||/\sum|F_o|$; $\langle \Delta\varphi \rangle_{cyl}$, final average phase shift; $\langle \Delta\varphi \rangle_{inv}$, average phase difference of final Fourier inversion; $\langle |\varphi_i - \varphi_f| \rangle$, average accumulated phase shift; correlation coefficient, $\langle F_oF_c \rangle / (\langle F_o^2 \rangle \langle F_c^2 \rangle)^{1/2}$.

By use of Wang's iterative solvent-flattening phase combination procedure with 2.8-Å resolution data and the refined structure of apo fragment 1, but with a shifted α-helix, three solvent masks (40% solvent) and 14 cycles of iterative phase determination and refinement using $(2|F_o| - |F_c|)$ maps were calculated and performed (Table II). The final 2.8-Å resolution $(2|F_o| - |F_c|)$ electron density map based on these phases clearly revealed the folding and tertiary structure of the whole Gla domain of $Ca^{2+}$ fragment 1 and the remainder of the fragment 1 structure. However, since the solvent was flattened, in order to better determine the initial phase angles of the structure, information concerning the location of possible $Ca^{2+}$ ions was initially necessarily compromised in the combined phases electron density map.

The 2.8-Å resolution ISIR–molecular replacement solvent-flattened structure was then partially refined by using restrained least-squares methods (Hendrickson & Konnert, 1980) with fairly stringent restraints on the parameters of the molecule and the diffraction pattern. The $R$ factor decreased

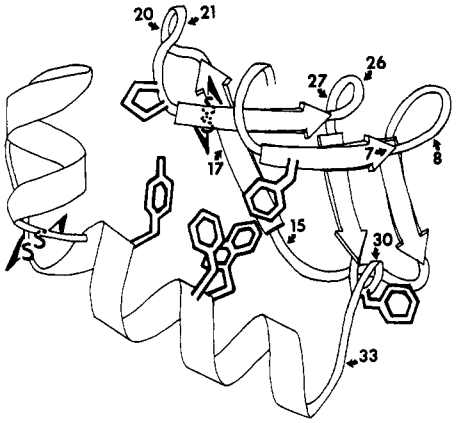


FIGURE 2: Ribbon drawing of the folding conformation of the Gla domain of fragment 1. Gla positions are numbered, aromatic residue side chains are shown (5, 29, 41, 42, and 45), and the accompanying tetradecapeptide disulfide loop (Cys48–Cys61) is also shown.

steadily during the course of alternately applying tighter and looser restraints from 0.44 to a value of 0.31. The latter included introduction of highly restrained individual $B$ values (basically individual residue $B$ values) during the last eight cycles. The refinement was halted at this convenient point to measure and process higher resolution intensity data (~2.0 Å). Electron density maps based on the refined 2.8-Å resolution ($2|F_o| - |F_c|$) coefficients and calculated phases were used to refit the structure, which is the one we report here. These electron and difference density maps based on calculated phase angles now had features that could be attributable to solvent and possibly $Ca^{2+}$ ion positions.

## Results and Discussion

*The Gla Domain.* The folding of the Gla domain is dominated by secondary structure: 3.0 turns of $\alpha$-helix (25%) and five $\beta$-strands (40%, for a total of about 65% secondary structure) arranged into two $\beta$-structural units stacked upon and at right angles to one another (Figure 2). In view of this high degree of organization, it would seem that *$Ca^{2+}$ ions induce the folding* and are responsible for the maintenance of the integrity of the Gla domain and that the disorder of the domain observed in apo fragment 1 might simply be the result of an unfolded chain in the absence of $Ca^{2+}$ ions. One of the $\beta$-units consists of two parallel strands, Gly4–Gla7 and Pro22–Arg25, while the other is made up of three strands: two adjacent parallel strands, Gla27–Phe29 and Arg10–Asn13, with, at the present stage of refinement, a more distantly arranged third strand, Arg16–Leu19, antiparallel to the former pair (Figure 2).

Another conspicuous aspect of the folding is the manner in which the disulfide of Cys18–Cys23 of the small conserved pentapeptide disulfide loop of Gla domains (Figure 1, Table I) approaches a cluster of conserved aromatic residues (Phe41, Trp42, Tyr45) formed by virtue of a turn of $\alpha$-helix (Figures 2 and 3). The resulting disulfide–aromatic $\pi$-electron interaction is probably responsible for the fluorescence quenching event generally observed to accompany $Ca^{2+}$ ion binding along with the conformational change demanded of membrane binding (Nelsestuen, 1976; Prendergast & Mann, 1977). Precedence for such a disulfide–$\pi$-electron interaction has already been established with the structure determination of a fluorescent probe $\alpha$-chymotrypsin–1-anilinonaphthalene-8-sulfonate complex (Weber et al., 1979), where it was shown that the naphthyl group of ANS binds at a single surface site of the enzyme and interacts intimately with the disulfide of Cys1–Cys122 at the N-terminus of the A-chain. The cluster of aromatic residues in the apo fragment 1 structure was puzzling and highly unusual (Tulinsky et al., 1988) in that the implication was they reside on the surface of the molecule and jut out into the solvent; however, in the crystal, they were the source of an important crystallographic 2-fold rotation packing interaction between independent molecules (Tulinsky & Park, 1988; Tulinsky et al., 1988). It now appears that these aromatic residues can function to help shield the Cys18–Cys23 disulfide bond from solvent in the folded Gla domain. In fact, calculations (Lee & Richards, 1971) show that the disulfides of the kringle of fragment 1 are equally inaccessible to solvent (Table III). Lastly, Phe5 of the Gla domain additionally reinforces the hydrophobic nature of the helical aromatic cluster as does Pro22, since proline is known to associate with such clusters (Tulinsky et al., 1973).

Table III: Accessible Area of Cysteines of $Ca^{2+}$ Fragment 1[a]

| residue | AA[b] | $(AA)_S$[c] | residue | AA[b] | $(AA)_S$[c] |
|---|---|---|---|---|---|
| 18 | 7.3 | 0.0 | 87 | 0.1 | 0.0 |
| 23 | 0.9 | 0.4 | 115 | 0.0 | 0.0 |
| 48 | 4.1 | 0.0 | 127 | 0.5 | 0.0 |
| 61 | 0.3 | 0.0 | 139 | 5.8 | 0.0 |
| 66 | 15.8 | 11.0 | 144 | 14.6 | 0.2 |

[a] Calculated according to the method of Lee and Richards (1971) with a sphere of radius 1.4 Å. [b] Accessible area in Å$^2$ for complete residue. [c] Accessible area in Å$^2$ for sulfur only.

The fluorescence quenching event caused by $Ca^{2+}$ ions binding to the bovine protein is actually biphasic with a fast (seconds) and a slower (minutes) component (Nelsestuen, 1976). It has been proposed that the former is the result of a conformational change involving a small population of Pro22 in a cis conformation and that the latter corresponds to the isomerization of trans Pro to the cis isomer (Marsh et al., 1979). The electron density in the vicinity of the tight Cys18–Cys23 loop is fairly crowded so that at present it is difficult to ascertain whether Pro22 is in a cis or trans con-

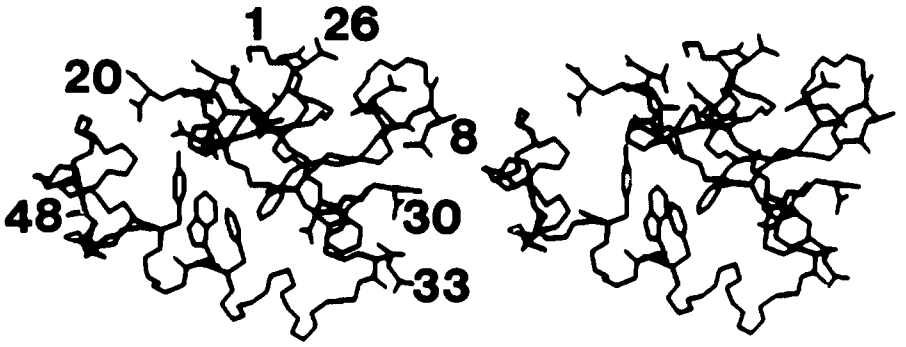


FIGURE 3: Stereoview of the CA, C, N structure of the Gla domain and the trailing disulfide loop. The aromatic cluster with Pro22 and the Gla side chains are also shown; selected residues are numbered for guidance.

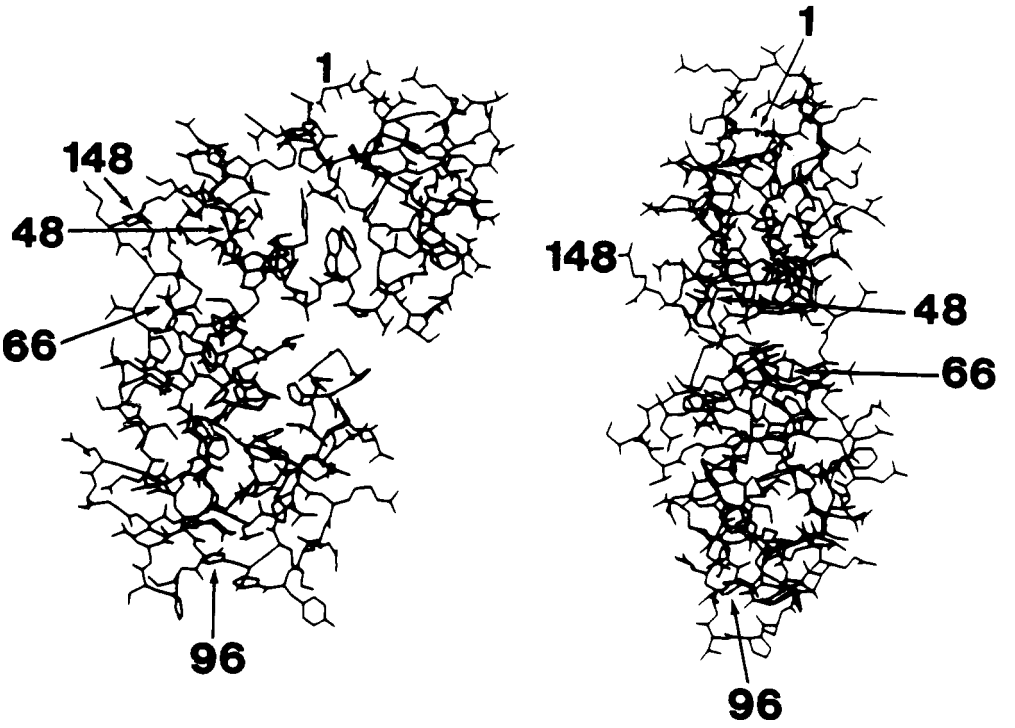


FIGURE 4: Complete tertiary structure of $Ca^{2+}$ fragment 1: left, viewed perpendicular to discoid faces (Gla domain, upper right above kringle domain); right, viewed edge-on to the discoid domains. Selected residues are numbered for guidance.

formation. However, this should be easy to establish at high resolution in the final stages of the refinement by omitting the Pro residue from least-squares calculations and examining $(2|F_o| - |F_c|)$ and difference electron density maps in the vicinity of the omission.

A stereoview of the folding of the Gla domain in $Ca^{2+}$ fragment 1 and its trailing tetradecapeptide (Cys48–Cys61) disulfide loop (Figure 1) is shown in Figure 3, from which it can be seen clearly that the Cys18–Cys23 disulfide is embedded in the region of the conserved aromatic cluster. Moreover, it will be seen that the Gla domain is relatively flat perpendicular to the $\beta$-structural features ($\sim$17–18 Å). Since the same applies to the kringle sequence, $Ca^{2+}$ fragment 1 approximates two coplanar discoids, one consisting of the Gla domain and its trailing tetradecapeptide disulfide loop and the other being the kringle, and the two are hinged together by a Leu62–Asn65 interdomain tetrapeptide link that can function as a point of flexibility. This can be seen from Figure 4 (left), from which the narrowed gap between the Gla and kringle domains ($\sim$5.0 Å) is also evident, originally observed in the apo fragment 1 structure to be about 8.5 Å (Tulinsky & Park, 1988; Tulinsky et al., 1988). The gap is lined on the Gla-domain side with its $\alpha$-helix, and the shift of the helix with $Ca^{2+}$ ion binding corresponds to about a 30° pivot. Since the active site of factor Xa in the prothrombinase complex is estimated to be about 69 Å above the surface of the membrane (Husten et al., 1987), the gap between domains in fragment 1, and most likely prothrombin, might be of functional significance in the complex to help position the cleavage site of prothrombin more precisely for catalysis with respect to the phospholipid membrane surface and the active site of factor Xa.

Since most of the Gla domain, like that of the kringle, is exposed to solvent through the discoid faces, it is not surprising that all the Gla residues of $Ca^{2+}$ fragment 1 are on the surface (Figure 3). On the other hand, the arrangement of the adjacent Gla residues (7–8, 20–21, 26–27) is somewhat suggestive, in that all but Gla8 line the top edge of the Gla domain along with Gla17 (Figures 2 and 3) and, thus, also the edge of the fragment 1 molecule (Figure 4). This creates a potentially intense electronegative environment in the molecule by virtue of the possibility of 12 charged carboxylate groups of the six Gla residues. The region might well be that of phospholipid binding, or related thereof, which interacts with negatively charged phosphate groups of the membrane through bridging $Ca^{2+}$ ions. It should be noted that the crystal structure appears highly relevant to solution observations because the intrinsic protein fluorescence of dissolved crystalline $Ca^{2+}$ fragment 1 was very similar to that observed for native fragment 1 fluorescence: $Ca^{2+}$ quenched protein fluorescence by about 50%.[3] Lastly, the other singly occurring Gla residues (15, 30, 33) also occur on the surface (Figure 3) and are readily accessible to solvent; however, there does not appear to be anything particularly systematic about their distribution in the domains as is the case of the paired Gla residues.

The Gla domain of $Ca^{2+}$ fragment 1 interacts and associates with its trailing disulfide loop to such an extent that the two together appear to form a three-dimensional structural unit. In fact, this disulfide loop projects off the last turn of the $\alpha$-helix of the Gla domain, thus concealing a turn of helix that would otherwise protrude from a compactly arranged Gla-domain structure. The $\alpha$-helix of the Gla domain and this disulfide loop appear to be an underlying frame upon which the remainder of the Gla domain anchors itself. It has been reported that the intrinsic fluorescence of 1–42 and 1–45 residue peptides of prothrombin is not quenched upon addition of $Ca^{2+}$ ion (Pollock et al., 1988), and it was suggested either that Trp42 does not have the same environment in the peptides as in fragment 1 or that Trp42 is not involved in the quenching process. Since the lack of quenching would seem to suggest lack of a conformational change, another possibility is that the structural support provided by the tetradecapeptide di-

[3] We thank Dr. G. L. Nelsestuen for carrying out this measurement.

sulfide loop is involved in the fluorescence change. However, notwithstanding, the phospholipid binding conformation appears to be attained since the 1–45 peptide has been shown to bind to phospholipid (Weber et al., 1988).

The chain from Phe5 to the N-terminal Ala1 is tucked in between the Cys18–Cys23 loop and the side chains of Gla26 and Gla27. Thus, accessibility of Ala1 is severely hindered from the solvent region. This agrees with the fact that, in $Ca^{2+}$ fragment 1, Ala1 is protected from acetylation (Welsch & Nelsestuen, 1988a). The observation that $Ca^{2+}$ ions in the presence of the Gly12–Lys44 peptide of prothrombin, which contains eight Gla residues, have no effect on the fluorescence of Trp42 and that the fragment does not bind to phospholipid suggests that the N-terminal region is important to the conformational change (Nelsestuen & Suttie, 1973). This is certainly consistent with the manner in which the Ala1 terminal is embedded in the surface protein matrix of the Gla domain. Carbohydrate-linked Asn101, which is fairly distant to the Gla domain, is also protected from acetylation by $Ca^{2+}$ ions (Welsch & Nelsestuen, 1988b). However, at present, there is no obvious crystallographic evidence to suggest the manner in which this might be accomplished.

It is of interest to note that of the N-terminal Gla-domain-containing proteins, a growth factor domain, which is a two-disulfide, double loop structure of about 20 residues with another decapeptide disulfide loop, generally follows the Gla domain except in the case of prothrombin and protein S, which have single disulfide loops. On the other hand, the growth factor proteins have a GlyAspGln insertion in the Gla domain immediately preceding the terminal half-cysteine (Table I) which probably increases the length of the $\alpha$-helix of the Gla domain by one turn (Tulinsky et al., 1988). Thus, with the growth factor proteins, the additional turn of helix could be expeditiously employed to support a larger two-disulfide, double loop structure of the growth factor at about a 45° angle to the Gla-domain $\alpha$-helix. The Gla-domain helix and an accompanying disulfide loop of the growth factor could then serve as a frame to maintain the remainder of the Gla-domain fold as in the case of $Ca^{2+}$ fragment 1. It is interesting to note that protein S, which does not have the tripeptide insertion (Table I), has only a single disulfide loop following the Gla domain as in prothrombin (Tulinsky et al., 1988). Even though the loop here is much larger than the tetradecapeptide loop of the latter, it is conceivable that it can serve the same supporting function for the Gla domain. However, if this is the case, the overall folding could be affected somewhat by Pro43, which effectively will put a bend in the $\alpha$-helix of protein S (Tulinsky et al., 1988).

*The Kringle Domain.* The kringle structure at the present stage of refinement is generally indistinguishable from that reported for the apoprotein (Tulinsky et al., 1988) with the carbohydrate remaining disordered in $Ca^{2+}$ fragment 1. The only difference from the apoprotein structure is in the C-terminal interkringle link region of the molecule, which has consistently displayed little density in $Ca^{2+}$ fragment 1 for this dodecapeptide. Refined phases have produced improved electron density in the C-terminal vicinity although it is not extensive enough to accommodate 12 residues and terminates at Arg148. Olsson et al. (1982) report the loss of five amino acids from the C-terminal during crystallization of $Ca^{2+}$ fragment 1. The lack of electron density might be confirming the proteolysis observation, which may be a reason for the lengthy growth period of $Ca^{2+}$ fragment 1 crystals.

*$Ca^{2+}$ Ions.* Although 2.8-Å resolution electron and difference density maps based on the partially refined phases now possess solvent features, none could be unambiguously interpreted and assigned to $Ca^{2+}$ ions. First, there were no outstandingly large electron density peaks in the vicinity of Gla side chains. In fact, not all the Gla side chains are themselves clearly fixed at this stage. Second, although there were many solvent peaks in the difference electron density, there were no outstandingly large ones corresponding to large $(2|F_o| - |F_c|)$ electron density near Gla residues. Therefore, rather than to speculate upon an ambiguous situation at this time, we defer the determination of the $Ca^{2+}$ ion positions to the high-resolution phase and refinement of this work.

## References


Bajaj, S. P., Butkowski, R. J., & Mann, K. G. (1975) *J. Biol. Chem. 250*, 2150–2156.

Bloom, J. W., & Mann, K. G. (1978) *Biochemistry 17*, 4430–4438.

Borowski, M., Furie, B. C., Bauminger, S., & Furie, B. (1986) *J. Biol. Chem. 261*, 14969–14975.

Dahlback, B., Lundwall, A., & Stenflo, J. (1986) *Proc. Natl. Acad. Sci. U.S.A. 83*, 4199–4203.

Deerfield, D. W., Olson, D. L., Berkowitz, P., Byrd, P. A., Koehler, K. A., Pedersen, L. G., & Hiskey, R. G. (1987a) *J. Biol. Chem. 262*, 4017–4023.

Deerfield, D. W., Olson, D. L., Berkowitz, P., Koehler, K. A., Pedersen, L. G., & Hiskey, R. G. (1987b) *Biochem. Biophys. Res. Commun. 144*, 520–527.

Degen, S. J. F., MacGillivray, R. T. A., & Davie, E. W. (1983) *Biochemistry 22*, 2087–2097.

Enfield, D. L., Ericsson, L. H., Fujikawa, K., Walsh, K. A., Neurath, H., & Titani, K. (1980) *Biochemistry 19*, 659–667.

Fernlund, P., & Stenflo, J. (1982) *J. Biol. Chem. 257*, 12170–12179.

Fung, M. R., Hay, C. W., & MacGillivray, R. T. A. (1985) *Proc. Natl. Acad. Sci. U.S.A. 82*, 3591–3595.

Hagen, F. S., Gray, C. L., O'Hara, P., Grant, F. J., Saari, G. C., Woodbury, R. G., Hart, C. E., Insley, M., Kisiel, W., Kurachi, K., & Davie, E. W. (1986) *Proc. Natl. Acad. Sci. U.S.A., 83*, 2412–2416.

Hendrickson, W. A., & Lattman, E. E. (1970) *Acta Crystallogr. B26*, 136–143.

Hendrickson, W. A., & Konnert, J. H. (1980) in *Computing in Crystallography* (Diamond, R., Ramaseshan, S., & Venkatesan, K., Eds.) pp 13.01–13.26, Indian Academy of Science, Bangalore, India.

Hojrup, P., Jensen, M. S., & Petersen, T. E. (1985) *FEBS Lett. 184*, 333–338.

Husten, E. J., Esmon, C. T., & Johnson, A. E. (1987) *J. Biol. Chem. 262*, 12953–12961.

Katayama, K., Ericsson, L. H., Enfield, D. L., Walsh, K. A., Neurath, H., Davie, E. W., & Titani, K. (1979) *Proc. Natl. Acad. Sci. U.S.A. 76*, 4990–4994.

Kurachi, K., & Davie, E. W. (1982) *Proc. Natl. Acad. Sci. U.S.A. 79*, 6461–6464.

Lee, B., & Richards, F. M. (1971) *J. Mol. Biol. 55*, 379–400.

Lundwall, A., Dackowski, W., Cohen, E., Shaffer, M., Mahr, A., Dahlback, B., Stenflo, J., & Wydro, R. (1986) *Proc. Natl. Acad. Sci. U.S.A. 83*, 6716–6720.

Magnusson, S., Petersen, T. E., Sottrup-Jensen, L., & Claeys, H. (1975) in *Proteases and Biological Control* (Reich, E., Rifkin, D. B., & Shaw, E., Eds.) pp 123–149, Cold Spring Harbor Laboratory, Cold Spring Harbor, NY.

Marsh, H. C., Scott, M. E., Hiskey, R. G., & Koehler, K. A. (1979) *Biochem. J. 183*, 513–517.

Nelsestuen, G. L. (1976) *J. Biol. Chem. 251*, 5648–5656.

Nelsestuen, G. L., & Suttie, J. W. (1973) *Proc. Natl. Acad. Sci. U.S.A. 70*, 3366-3370.
Nelsestuen, G. L., Zytkovicz, T. H., & Howard, J. B. (1974) *J. Biol. Chem. 249*, 6347-6350.
Nelsestuen, G. L., Resnick, R. M., Wei, G. J., Pletcher, C. H., & Bloomfield, V. A. (1981) *Biochemistry 20*, 351-358.
Olsson, G., Andersen, L., Lindqvist, O., Sjolin, L., Magnusson, S., Petersen, T. E., & Sottrup-Jensen, L. (1982) *FEBS Lett. 145*, 317-322.
Plutzky, J., Hoskins, J. A., Long, G. L., & Crabtree, G. R. (1986) *Proc. Natl. Acad. Sci. U.S.A. 83*, 546-550.
Pollock, J. S., Shepard, A. J., Weber, D. J., Olson, D. L., Klapper, D. G., Pedersen, L. G., & Hiskey, R. G. (1988) *J. Biol. Chem. 263*, 14216-14223.
Predergast, F. G., & Mann, K. G. (1977) *J. Biol. Chem. 252*, 840-850.
Stenflo, J., Fernlund, P., Egan, W., & Roepstorff, P. (1974) *Proc. Natl. Acad. Sci. U.S.A. 71*, 2730-2733.
Tulinsky, A., & Park, C. H. (1988) in *Current Advances in Vitamin K Research* (Suttie, J. W., Ed.) pp 295-304, Elsevier Science Publishing Co., New York.
Tulinsky, A., Vandlen, R. L., Morimoto, C. N., Mani, N. V., & Wright, L. H. (1973) *Biochemistry 12*, 4185-4192.
Tulinsky, A., Park, C. H., & Rydel, T. J. (1985) *J. Biol. Chem. 260*, 10771-10778.
Tulinsky, A., Park, C. H., & Skrzypczak-Jankun, E. (1988) *J. Mol. Biol. 203*, 885-901.
Wang, B. C. (1985) *Methods Enzymol.* 115 (Part B), 90-112.
Weber, D. J., Pollock, J. S., Pedersen, L. G., & Hiskey, R. G. (1988) *Biochem. Biophys. Res. Commun. 155*, 230-235.
Weber, L. D., Tulinsky, A., Johnson, J. D., & El-Bayoumi, M. A. (1979) *Biochemistry 18*, 1297-1303.
Welsch, D. J., & Nelsestuen, G. L. (1988a) *Biochemistry 27*, 4939-4945.
Welsch, D. J., & Nelsestuen, G. L. (1988b) *Biochemistry 27*, 4946-4952.

## *Articles*

# Purification and Steady-State Kinetic Characterization of Human Liver $\beta_3\beta_3$ Alcohol Dehydrogenase†

Joe C. Burnell, Ting-Kai Li, and William F. Bosron*

*Departments of Biochemistry and Medicine, Indiana University School of Medicine, Indianapolis, Indiana 46223*

*Received December 30, 1988; Revised Manuscript Received May 3, 1989*

ABSTRACT: Human liver alcohol dehydrogenase catalyzes the $NAD^+$-dependent oxidation of alcohols. Isoenzymes are produced in liver by five different genes, two of which are polymorphic. We have studied the three $\beta\beta$ isoenzymes produced at *ADH2* because they exhibit very different kinetic properties and they appear with different frequencies in different racial populations. The $\beta_3\beta_3$ isoenzyme which appears in 25% of black Americans was purified to homogeneity, and conditions were found to stabilize this labile isoenzyme. The comparison of substrate specificity among $\beta\beta$ isoenzymes for primary straight-chain alcohols indicates that there is a positive correlation between $V_{max}/K_M$ and the log octanol/water partition coefficient for alcohols with $\beta_2\beta_2$ and $\beta_3\beta_3$ but not with $\beta_1\beta_1$. Methyl substitutions at C1 or C2 of these alcohols reduce the catalytic efficiency with all three isoenzymes. The $K_M$ and $K_i$ values of $\beta_3\beta_3$ for $NAD^+$ and NADH are substantially higher than values for $\beta_1\beta_1$ or $\beta_2\beta_2$. The $V_{max}$ of $\beta_3\beta_3$ for ethanol oxidation is 90 times that of $\beta_1\beta_1$. Sequencing of the $\beta_3$ subunit and gene indicates that the polymorphism results from a single amino acid exchange of Cys-369 in $\beta_3$ for Arg-369 in $\beta_1$ and $\beta_2$ [Burnell et al. (1987) *Biochem. Biophys. Res. Commun. 146*, 1227-1233]. In horse alcohol dehydrogenase and $\beta_1\beta_1$, the guanidino group of Arg-369 is thought to stabilize the NAD(H)-enzyme complex by bonding to one of the pyrophosphate oxygens. Thus, the substitution of Cys-369 in $\beta_3\beta_3$ explains its weak binding of coenzymes and high activity.

The majority of ingested ethanol is metabolized in the liver through acetaldehyde, to acetate. The rate-limiting step in this process is the oxidation of ethanol to acetaldehyde which is catalyzed by the $NAD^+$-dependent alcohol dehydrogenase (ADH, EC 1.1.1.1). In human liver, this enzyme exists in multiple molecular forms which are the products of five genes. The subunits encoded by *ADH1* ($\alpha$), *ADH2* ($\beta$), and *ADH3* ($\gamma$) form homodimeric and heterodimeric class I ADH isoenzymes (Vallee & Bazzone, 1983; Smith, 1986; Bosron & Li, 1987). Polymorphism has been observed at two of these loci, resulting in the production of three different $\beta$ subunits, $\beta_1$, $\beta_2$, and $\beta_3$ (Smith et al., 1971; Bosron et al., 1983a), and two different $\gamma$ subunits, $\gamma_1$ and $\gamma_2$ (Smith et al., 1972). It has been proposed that differences in the catalytic properties of these polymorphic liver ADH isoenzymes may account for part of the observed genetic variability of ethanol metabolic rate in humans (Bosron & Li, 1981, 1987).

We have focused our recent efforts on the catalytic and structural characterization of the $\beta\beta$ isoenzymes because they exhibit widely different kinetic properties and appear with different frequencies in different racial groups. $\beta_1$ is found

†This work was supported by National Institute on Alcohol Abuse and Alcoholism Research Grant AA02342 and Training Grant AA07462.
*Address correspondence to this author at the Department of Biochemistry, Indiana University School of Medicine.

0006-2960/89/0428-6810$01.50/0 